

https://doi.org/10.1070/QEL18018

Broadband emission from polycrystalline graphite

S.Sh. Rekhviashvili, D.S. Gaev, Z.Ch. Margushev

Abstract. **Visible radiation spectra of polycrystalline graphite under electrical and laser excitation is studied. It is shown that two different mechanisms of photon emission with a broadband spectrum are implemented in this material. The radiation arising as a result of resistive heating is thermal radiation, whose parameters are close to those of blackbody radiation. The laser-induced secondary radiation in the visible range is anti-Stokes luminescence. A red shift of the laser-induced radiation from fine-grained graphite with respect to the similar spectrum of a bulk sample is observed.**

Keywords: *polycrystalline graphite, broadband emission, thermal radiation, anti-Stokes luminescence, stimulated Raman scattering.*

1. Introduction

The physical properties of carbon nanomaterials have been actively studied in view of their high application potential in electronics and engineering. Particular attention is paid to the problems related to the emission from carbon nanomaterials. The reason is that these materials have already become indispensable for high-temperature nanophotonics in the visible and IR ranges.

Light can be generated in carbon nanomaterials using electric current and electromagnetic impacts. For example, the electroluminescence of fullerenes and carbon nanotubes was investigated in [1–12]. Broadband emission of fullerene crystals was found in [1, 2]. Electroluminescence was observed in samples with a high electrical conductivity. The luminescence intensity depends nonlinearly on the current value. The electrical conductivity increases irreversibly at large current values. The radiation output increases, and the threshold current value, corresponding to the onset of phonon emission, increases. This is somewhat similar to the effect of current pinching and may indicate the thermal nature of radiation. Radiation with similar properties was also observed in composites of polymer–fullerene type [3, 9]. A comparison of the carbon nanotube electroluminescence with blackbody radiation was performed in [4–7, 11, 12]. Several factors were proposed to explain the electroluminescence: thermal radiation [4–6, 11], photonic bandgap effect [7], generation of excitons, radiative electron–hole transitions, and Van Hove features [11, 12]. The electroluminescence of graphene and structures on its basis was investigated later in many studies (see, e. g., [13–21]). Attention was paid to the role of interband transitions; electron tunnelling [14, 16]; and, again, thermal radiation [17–20]. Unfortunately, a transparent physical mechanism of the emission from carbon nanomaterials under electric current impact has not been elaborated yet.

Currently, the most widespread method in this field is the detection of electroluminescence of carbon nanotubes and graphene in structures of channel-embedded field-effect transistor type [9–12, 18–21]. This technique is of interest from applied point of view, because graphene emission is considered to be a highly efficient way to cool graphene-based high-speed transistors. Another fairly informative method for studying the electroluminescence of graphene is scanning tunnel microscopy [14, 16, 21].

The laser-induced emission and photoluminescence spectra of carbon nanomaterials were studied in [22–35]. The emission of fullerenes was investigated in [22–28]. Laser irradiation of polycrystalline fullerite C_{60} with power exceeding some threshold value leads to the occurrence of 'white' broadband radiation. The exciton mechanism of generation is suggested to occur [22, 23]. At high laser intensities one can observe a sharp increase in the exciton lifetime, as well as a red shift and broadening of secondary radiation spectra. The high recombination time of triplet excitons leads to accumulation of photoexcited carriers. During photon absorption transitions of charge carriers to high energy levels may occur in two or more stages. The additional recombination of carriers occupying these levels is apparently one of the reasons for the spectral broadening. The specific features of fullerene emission in different environments were considered in [24–28].

Of greatest practical interest are the experimental results on laser-induced emission of nanotubes and graphenes [29–35]. The laser heating and emission of samples with carbon nanotubes were investigated in [29–31]. Even a weak laser effect with intensity of $\sim$1 kW cm^{-2} causes bright luminescence of the samples [29]. No emission from bulk graphite and amorphous carbon was observed under the same conditions. A noteworthy fact is the influence of external atmosphere: an increase in air pressure reduces the secondary radiation intensity [31]. The secondary radiation vanishes at the aforementioned laser beam intensity and a pressure of 1000 Pa. This is explained by the convective heat exchange and indicates the thermal nature of the process. It was suggested in

S.Sh. Rekhviashvili Institute of Applied Mathematics and Automation, Kabardino-Balkarian Scientific Center, Russian Academy of Sciences, ul. Shortanova 89A, 360000 Nalchik, Kabardino-Balkarian Republic, Russia; e-mail: rsergo@mail.ru;
D.S. Gaev Berbekov Kabardino-Balkarian State University, ul. Chernyshevskogo 173, 360004 Nalchik, Russia;
Z.Ch. Margushev Institute of Informatics and Problems of Regional Management, Kabardino-Balkarian Scientific Center, Russian Academy of Sciences, ul. I. Armand 37a, 360000 Nalchik, Kabardino-Balkarian Republic, Russia

Received 7 September 2021; revision received 17 November 2021
Kvantovaya Elektronika **52** (4) 382–385 (2022)
Translated by Yu.P. Sin'kov

[29] that the high efficiency of sample heating is mainly due to weak heat scattering and low specific heat of nanotubes. The wide spectra measured in [29–31] correspond to the blackbody radiation at temperatures of 1200–2500 K.

The spectra of laser-induced emission from graphene, graphene foam, and graphene ceramics were measured in [32–35]. The results obtained are on the whole in agreement with the corresponding data on nanotubes. The luminescence temperature of graphene, estimated from the Planck formula, exceeds 3000 K [32]. For graphene foam, wide emission bands in the visible and IR ranges were observed at high laser excitation intensities [35]. The luminescence area is limited by the focal spot sizes. As in the case of nanotubes, one can observe a dependence of the emission intensity on the atmospheric pressure.

A common characteristic of the emission from all carbon nanomaterials is the existence of broadband spectra, whose nature has not been completely understood yet. Experiments on an appropriate model object may help understand more deeply the physical pattern of broadband emission of all carbon nanomaterials. Polycrystalline graphite, which consists of randomly oriented crystallites, may play the role of this object. This material can be used both in the form of a bulk solid and as a fine-grained (e. g., mechanically ground) powder. In this paper, we report the results of studying the emission spectra of polycrystalline graphite, aimed at revealing the physical mechanisms of emission of carbon materials and nanomaterials.

2. Experimental

The experiment was performed using graphitised EGSP-1 electrodes (length 3 cm, cross section 2×2 mm^2, resistivity 5.5×10^{-6} Ω m, density 1.65 g cm^{-3}). Both bulky and mechanically ground samples were investigated; the average particle size in powder samples was less than 1 μm. Emission in the visible range was obtained by resistive heating of electrodes or IR laser irradiation of electrodes and fine-grained powder. Resistive heating was performed only in air. Laser irradiation was carried out either in air or in vacuum. Some samples were placed in a glass ampoule, evacuated and sealed to a residual pressure of $\sim10^{-4}$ Torr. Thermal emission spectra of tungsten wire were also measured for comparison.

Resistive heating was performed using an adjustable autotransformer with voltage and current of 15 V and 8 A, respectively. Resistive heating was carried out at different heat release powers in the sample, up to the limiting temperature, corresponding to the electrode burning out. The radiation source was a cw Ti : sapphire laser Fusion, generating 800-nm radiation with a beam diameter of 2 mm. The output laser power was 0.3 W; monitoring was performed with an S142C device. The laser beam was focused by an aspherical lens into a spot 4 μm in diameter. The irradiated portion of the sample was placed exactly at the lens focal spot. The total radiation intensity was 2.4×10^6 W cm^{-2}. To exclude evaporation and ionisation of samples, the laser beam intensity was reduced by three orders of magnitude by reducing the laser pump power and replacing the focusing lenses. The emission spectra were recorded by an HR4000 spectrometer with a fibre input in the "Intensity" spectrum recording mode.

3. Discussion

Figures 1 and 2 show the emission spectra of polycrystalline graphite. One can see a significant difference in the positions of spectral bands, depending on the excitation method. Upon resistive heating bulk polycrystalline graphite obeys Wien's displacement law, which indicates directly the thermal mechanism of emission. The temperatures for curves (*4*), (*3*), and (*2*) in Fig. 1, estimated from the formula $T = 2.898\times10^{-3}/\lambda_{max}$, where λ_{max} is the radiation wavelength with maximum intensity, are, respectively, 3600, 3700, and 3800 °C. Above 3800 °C emission spectra could not be measured because of the fast electrothermal destruction of electrodes.

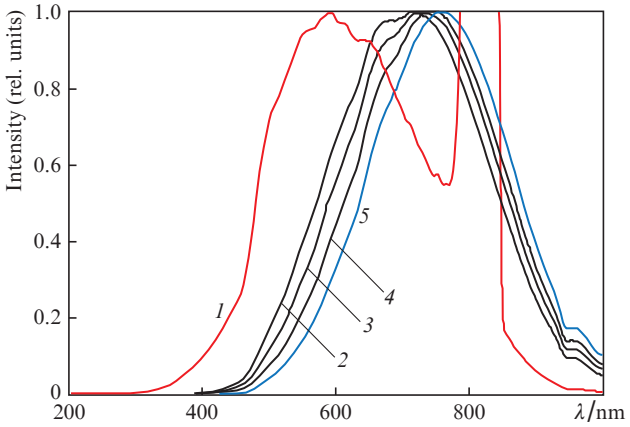

Figure 1. (Colour online) Spectra of laser-induced emission (*1*) and emission caused by resistive heating at different temperatures (*2*, *3*, *4*) of bulk polycrystalline graphite and (for comparison) thermal emission spectrum of a tungsten wire near its melting temperature (*5*).

The laser-induced radiation has radically different properties. A variation in the external IR laser intensity within three orders of magnitude affects only the brightness of visible luminescence but does not affect the position of the spectral band, which is centred at 590–595 nm. The colour temperature of this secondary radiation is ~4640 °C, a value 100 °C larger than the melting (sublimation) temperature of crystalline graphite [36]. All these facts indicate the occurrence of luminescence in the material. The transition from continuous to fine-grained material is accompanied by a red shift of the emission spectrum. The shift (determined from the peak positions) is as high as 60 nm, as can be seen in Fig. 2.

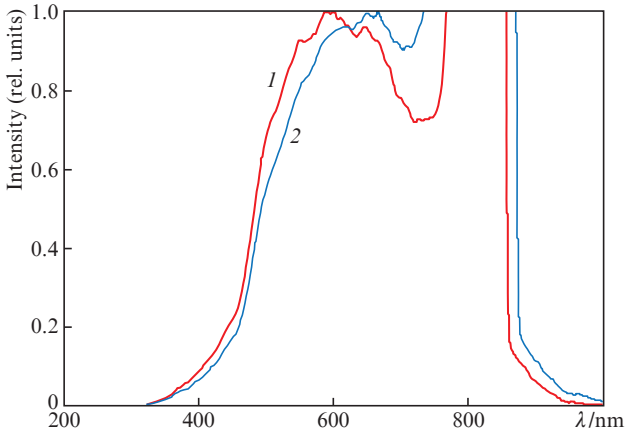

Figure 2. (Colour online) Emission spectra of (*1*) bulk and (*2*) fine-grained samples of polycrystalline graphite.

When performing measurements in air and in vacuum, the position and general view of the spectral bands remain the same. It should also be noted that the shape of the emission spectra of fine-grained graphite powder practically coincides with that of the emission spectra of graphene foam and ceramics [33–35].

In our opinion, the experimental results of this study, as well as the known data in the literature of the laser-induced emission of carbon nanomaterials, are indicative of stimulated Raman scattering as the mechanism of anti-Stokes luminescence. According to [37], the signs of stimulated Raman scattering in our case are as follows: (1) there is an intensity threshold for the excitation IR laser radiation, (2) there is only one band with several pronounced symmetric harmonics in the spectra, (3) the width of spectral bands covers the range of Raman (Stokes) shifts for crystalline graphite and graphene [38], and (4) the spectra are narrowed near the maxima. Two wide bands of laser-induced emission of graphene foam in the visible and short-wavelength IR regions were measured in [35]. According to our interpretation, these bands are due to the anti-Stokes and Stokes scattering components.

Carbon materials are highly susceptible to laser heating because of their high absorptivity; thermal energy is accumulated in them for a short time, and then this energy is transformed into the anti-Stokes luminescence. An excitation photon is absorbed, and a mobile exciton is formed in the initial stage. The next intermediate quantum state arises when the exciton absorbs a nonequilibrium phonon. Further recombination of this exciton occurs with de-excitation of a scattered photon having a higher frequency. Experiments show that this process occurs qualitatively in the same way in both bulk and dispersed samples, but in different frequency ranges of photons and phonons. A red shift of the emission spectrum is observed (Fig. 2), which, by analogy with the shift of the 2D Raman band in graphite, is explained by the weakening of the electron–phonon interaction and, therefore, decrease in the degree of macroscopic polarisation.

We explain also the luminescence spectral broadening by possible singlet–triplet splitting of exciton levels and additional transitions between higher exciton levels.

Note that an increase in the resistive heating temperature leads to the occurrence of new harmonics in the emission spectrum, which manifest themselves as additional diffuse peaks [Fig. 1, bands (*2–4*)], and the shape of the spectra becomes similar to that of the laser-induced emission spectra. In our interpretation, this is explained by the enhancement of electron–phonon interaction at large values of electric current density and temperature. Concerning carbon nanomaterials, extremely strong electric fields are implemented in them initially; therefore, electroluminescence may also occur in this case due to the stimulated Raman scattering.

4. Conclusions

The results of this study make it possible to understand better the nature of broadband emission from carbon materials and nanomaterials. It is shown by an example of polycrystalline graphite that two radically different types of radiation may arise in the same carbon material: thermal radiation and anti-Stokes luminescence.

The laser-induced emission spectra are found to be red-shifted when passing from solid to fine-grained polycrystalline graphite. This phenomenon is explained by the change in the macroscopic polarisability and is not related to the quantum confinement in limited structures, which exhibit a blue shift. The laser-induced emission spectrum of fine-grained polycrystalline graphite has a characteristic maximum at a wavelength of $\sim$650 nm, which is typical of different carbon nanomaterials.

It follows from the obtained experimental results that the existing mathematical models of IR laser heating, which take into account the radiative heat exchange in terms of the Stefan–Boltzmann law, are incorrect for graphite and different carbon nanomaterials and must be improved significantly.

References

1. Werner A.T., Byrne H.J., O'Brien D.F., Roth S. *Proc. SPIE*, **2284** (1994); https://doi.org/10.1117/12.196129.
2. Werner A.T., Byrne H.J., Roth S. *Synthetic Metals*, **70**, 1409 (1995).
3. Werner A.T., Grem G., Byrne H.J., Leising G., Roth S. *Mater. Sci. Forum*, **191**, 195 (1995).
4. Sveningsson M., Jonsson M., Nerushev O.A., Rohmund F., Campbell E.E.B. *Appl. Phys. Lett.*, **81**, 1095 (2002).
5. Li P., Jiang K., Liu M., Li Q., Fan S. *Appl. Phys. Lett.*, **82**, 1763 (2003).
6. Wei J., Zhu H., Wu D. *Appl. Phys. Lett.*, **84**, 4869 (2004).
7. Zhao Z.G., Li F., Liu C., Cheng H.M. *J. Appl. Phys.*, **98**, 044306 (2005).
8. Freitag M., Tersoff J., Chen J., Tsang J., Avouris P. *AIP Conf. Proc.*, **786**, 477 (2005).
9. Kim H., Kim J.Y., Park S.H., Lee K. *Appl. Phys. Lett.*, **86**, 183502 (2005).
10. Marquardt C.W., Grunder S., Błaszczyk A., Dehm S., Hennrich F., von Lohneysen H., Mayor M., Krupke R. *Nat. Nanotechnol.*, **5**, 863 (2010).
11. Liu Z., Bushmaker A., Aykol M., Cronin S.B. *ACS Nano*, **5** (6), 4634 (2011).
12. Janas D., Czechowski N., Krajnik B., Mackowski S., Koziol K.K. *Appl. Phys. Lett.*, **102**, 181104 (2013).
13. Freitag M., Chiu H.Y., Steiner M., Perebeinos V., Avouris Ph. *Nature Nanotech.*, **5**, 497 (2010).
14. Beams R., Bharadwaj P., Novotny L. *Nanotechnology*, **25** (5), 055206 (2014).
15. Kwon W., Kim Y.-H., Lee C.-L., Lee M., Choi H.C., Lee T.-W., Rhee S.-W. *Nano Lett.*, **14**, 1306 (2014).
16. Chong M.C., Afshar-Imani N., Scheurer F., Cardoso C., Ferretti A., Prezzi D., Schull G. *Nano Lett.*, **18**, 175 (2018).
17. Dong H.M., Xu W., Peeters F.M. *Opt. Express*, **26** (19), 24621 (2018).
18. Yang J., Du W., Su Y., Gong S., He S., Ma Y. *Nat. Commun.*, **9**, 4033 (2018).
19. Luo F., Fan Y., Peng G., Xu Sh., Yang Y., Yuan K., Liu J., Ma W., Xu W., Zhu Z.H., Zhang X., Mishchenko A., Ye Y., Huang H., Han Z., Ren W., Novoselov K.S., Zhu M., Qin S. *ACS Photonics*, **6** (8), 2117 (2019).
20. Baudin E., Voisin Ch., Placais B. *Adv. Funct. Mater.*, **30** (8), 1904783 (2020).
21. Junaid M., Md Khir M.H., Witjaksono G., Ullah Z., Tansu N., Saheed M.S.M., Kumar P., Hing Wah L., Magsi S.A., Siddiqui M.A. *Molecules*, **25**, 4217 (2020).
22. Feldmann J., Fischer R., Guss W., Gobel E., Schmitt-Rink S., Kratschmer W. *Europhys. Lett.*, **20**, 553 (1992).
23. Byrne H., Maser W., Ruhle W., Mittelbach A., Roth S. *J. Appl. Phys. A*, **56**, 235 (1993).
24. Sibley S.P., Argentine S.M., Francis A.H. *Chem. Phys. Lett.*, **188**, 187 (1992).
25. Shin E., Park L., Lee M., Kim D., Suh Y.D., Yang S.I., Jin S.M., Kim S.K. *Chem. Phys. Lett.*, **209**, 427 (1993).
26. Palewska K., Sworakowski J., Chojnacki H. *J. Phys. Chem.*, **97**, 12167 (1993).
27. Zhu L., Li Y., Wang J., Shen J. *J. Appl. Phys.*, **77**, 2801 (1995).
28. Bayramov A.I., Mamedov N.T., Dzhafarov T.D., Aliyeva Y.N., Ahmadova K.N., Alizade E.H., Asadullayeva S.Q., Sadigov M.S., Ragimov S.K. *Thin Solid Films*, **690**, 137566 (2019).

29. Zeng H., Yang C., Dai J., Cui X. *J. Phys. Chem. C.*, **112** (11), 4172 (2008).
30. Lim Z.H., Lee A., Zhu Y., Lim K.-Y., Sow C.-H. *Appl. Phys. Lett.*, **94**, 073106 (2009).
31. Lim Z.H., Lee A., Lim K.Y.Y., Zhu Y., Sow C.-H. *J. Appl. Phys.*, **107**, 064319 (2010).
32. Lui C.H., Mak K.F., Shan J., Heinz T.F. *Phys. Rev. Lett.*, **105**, 127404 (2010).
33. Strek W., Tomala R., Lukaszewicz M., Cichy B., Gerasymchuk Y., Gluchowski P., Marciniak L., Bednarkiewicz A., Hreniak D. *Sci. Rep.*, **7**, 41281 (2017).
34. Strek W., Cichy B., Radosinski L., Gluchowski P., Marciniak L., Lukaszewicz M., Hreniak D. *Light Sci. Appl.*, **4**, 237 (2015).
35. Strek W., Tomala R. *Phys. B: Condens. Matter*, **579**, 411840 (2020).
36. Savvatimskiy A.I. *Carbon*, **43** (6), 1115 (2005).
37. Zubov V.A., Sushinskii M.M., Shuvalov I.K. *Sov. Phys. Usp.*, **7** (3), 419 (1964) [*Usp. Fiz. Nauk*, **83** (2), 197 (1964)].
38. Ferrari A.C. *Solid State Commun.*, **143**, 47 (2007).